Available online at www.sciencedirect.com
SCIENCE DIRECT®
Inorganica Chimica Acta 357 (2004) 689–698
Inorganica Chimica Acta
www.elsevier.com/locate/ica

Formation and structural studies of iron(III) and ruthenium(II) complexes of 1,4,7-triazacyclononane and *N*-monofunctionalised 1,4,7-triazacyclononane

Andrew L. Gott, Patrick C. McGowan *, Thomas J. Podesta, Christopher W. Tate

Department of Chemistry, University of Leeds, Leeds LS2 9JT, UK

Received 23 April 2003; accepted 8 July 2003

Abstract

A series of 1,4,7-triazacyclononane derivatives of Fe(III) and Ru(II) have been investigated. The objective of this work was to investigate the effect of changing the functionality of a pendant group in order to create different Ru(II) and Fe(III) environments. From these studies, some interesting features are elucidated and different stacking properties arise due to the intra- and intermolecular X–H···Cl (X = O, N) interactions for the Fe(III) and Ru(II) complexes.

1. Introduction

Several naturally occurring enzymes have been found to contain an iron–oxygen–iron arrangement [1–3]. Many compounds have been synthesised in an attempt to model this type of motif, using several types of ligand system to 'cap' the ends of the metal core [4]. On a related theme, there have been some papers published on modelling the extradiol oxidative cleavage of catechol by the iron enzymes catechol dioxygenases [5–9]. Reported in one paper is the use of $FeCl_2$/tacn/pyridine/O_2/MeOH mixture in the extradiol ring cleavage [9]. A number of reactive intermediates have been purported for these types of reactions and the results reported in this paper may have some bearing on possible intermediates in the reaction mechanism [9].

Work on ruthenium tacn complexes has been driven by interest in terms of their coordination chemistry, redox behaviour and electrochemistry, and also as a spectator ligand in the study of "non-innocent" donor ligands [10–13]. Also, the chemistry of a wide range of organometallic compounds containing the ruthenium tacn moiety have been investigated [14–16], which can exhibit catalytic properties in a variety of systems, including the selective oxidation of alcohols and ketones [17,18].

Herein we report the synthesis and structural studies of a number of Fe(III)μ-oxo derivatives chloride *N*-monofunctionalised 1,4,7-triazacyclononane systems. Variation of the coordinating capability of the pendant arm has a dramatic effect on the structure of the oxidised Fe(III) species. One of the Fe(II) precursors to these compounds has been published previously [19] and here this paper represents an exploration into some of the reactivity of the Fe(II) complexes and formation of new Ru(II) complexes. Not only is the discovery of new synthetic routes for ruthenium tacn important but controlling the reaction conditions to produce the desired product is crucial. One of the controlling mechanisms is the reliance on the hydrogen bonding capability of the N–H groups of the triazacyclononane ligand in transition metal complexes [20].

2. Results and discussion

2.1. Synthesis and characterisation

The iron(III) tacn derivatives can be synthesised through one of two methods. The compound [bis(1-(2-methylpyridyl)-1,4,7-triazacyclononane iron(III)chloride)-

---

* Corresponding author. Fax: +44-0113-2336565.
E-mail address: p.c.mcgowan@chem.leeds.ac.uk (P.C. McGowan).

0020-1693/$ - see front matter © 2003 Elsevier B.V. All rights reserved.
doi:10.1016/j.ica.2003.07.002

μ-oxo]dichloride (**1**), was synthesised by stirring a solution of [1-(2-methylpyridyl)-1,4,7-triazacyclononane]iron(II)-dichloride in dichloromethane overnight in air (Scheme 1). During this time the product precipitated from the solution as a brown powder, which was isolated by filtration. Compound **1** was characterised by microanalysis, mass spectrometry, infrared spectroscopy and X-ray crystallography.

The compound bis[1-(prop-3-ene)-1,4,7-triazacyclononane iron(III)dichloride]μ-oxide (**2**), was prepared by heating a suspension of anhydrous iron(II) chloride in THF with a solution of 1-(propene)-1,4,7-triazacyclononane to reflux for 7 days in air (Scheme 2). The solvent was removed under reduced pressure and the product extracted with dichloromethane. The product was obtained as a green powder upon removal of the dichloromethane. The product was characterised by microanalysis, infrared spectroscopy, mass spectrometry and X-ray crystallography. Green crystals of **2**, suitable for X-ray diffraction were grown by diffusing petrol into a dichloromethane solution of the compound. After repeated attempts, the isolation of the Fe(II) product with 1-(propene)-1,4,7-triazacyclononane did not prove possible.

Magnetic susceptibility measurements on compounds **1** and **2** have been recorded. Measurements were made at 294.5 K. The observed μ_{eff} for both compounds are 2.81 and 2.03 BM, respectively. The data show that both compounds are antiferromagnetically coupled. The values of μ_{eff} are consistent with previously reported examples [3]. Observed in the infrared spectrum for both complexes is an intense band at $\nu = 801$ cm^{-1} for **1** and $\nu = 806$ cm^{-1} for **2**. This is assigned to the band ν_{as} Fe–O–Fe and is characteristic for μ-oxo bridged iron complexes [3].

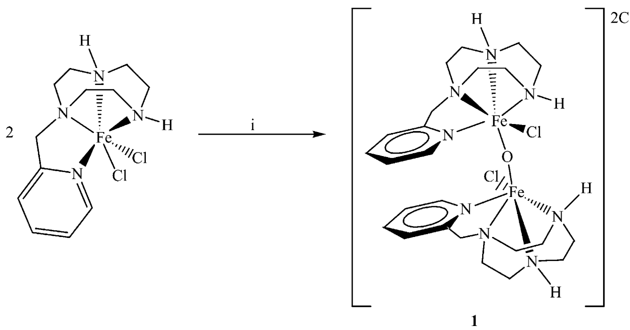

Scheme 1. Reagents and conditions, (i) O_2/DCM.

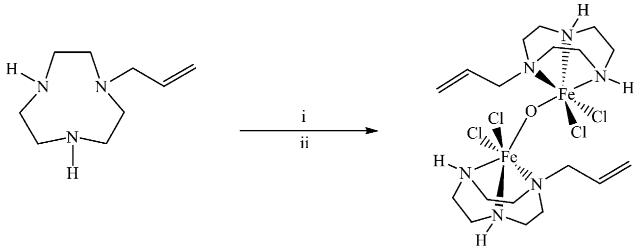

Scheme 2. Reagents and conditions, (i) THF, (ii) O_2/$FeCl_2$.

It is interesting to compare complexes **1** and **2**. For complex **1**, the nitrogen remains bound to the iron centre after oxidation leading to the formation of a dicationic binuclear complex. Complex **2** is different since the pendant alkene arms do not interact with the either of the metal centres and the oxidised complex is neutral. The most prominent feature of the two complexes is the iron–oxygen–iron core. This type of bridging arrangement is commonly found in bio- and experimental inorganic chemistry. Among these systems, there are several examples of triazacyclononane ligands being used. Most of the model complexes synthesised contain not only the bridging oxygen atom, but also one or two bridging types, such as μ-hydroxyl, μ-carboxylato and μ-acetato [21–24]. There are fewer examples of systems with only one oxygen atom bridging the two iron centres, and even fewer involving a triazacyclononane bridging ligand [3].

To broaden the scope of reactivity and different binding modes of the tacn ligands, a series of ruthenium complexes were synthesised. It was observed that the reaction of (1-(2-methylpyridyl)-1,4,7-triazacyclononane) and $RuCl_2(PMePh_2)_4$ in toluene at room temperature gave no product and this is different to an analogous reaction with $RuCl_2(PPh_3)_3$ [19]. The reaction proceeds at the reflux temperature of toluene and the desired product **3** is formed according to Scheme 3. Complex **3** was characterised by NMR spectroscopy, mass spectrometry, microanalysis and X-ray crystallography. This observation can be rationalised by the increased coordination number of the ruthenium starting material, which is six coordinate and therefore there is no coordination site in which the ligand can initially attach itself. In this case, it requires a higher reaction temperature with which to labilise one of the phosphine ligands.

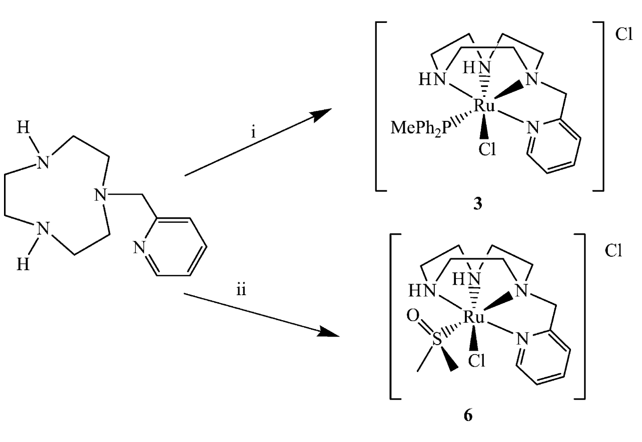

Scheme 3. Reagents and conditions, (i) toluene/reflux 30 min/ $RuCl_2(PPh_2Me)$, (ii) toluene/reflux 1 h/$RuCl_2(DMSO)_4$.

This phenomenon is not reflected in the chemistry of unfunctionalised tacn, where the reaction of tacn with $RuCl_2(PMePh_2)_4$, and $RuCl_2(PMe_2Ph)_4$ both proceed at room temperature to yield complexes $[(tacn)RuCl(PMePh_2)_2]Cl$ (**4**) and $[(tacn)RuCl(PMe_2Ph)_2]Cl$ (**5**), respectively. But, it was observed that the formation of complex **5** is less facile than **4**, presumably due to the stability of the starting material with respect to dissociation of the phosphine ligands. Complexes **4** and **5** were both characterised by NMR spectroscopy, mass spectrometry and elemental analysis. The attempted formation of $[(tacn)RuCl(PMe_3)_2]Cl$ proved impossible, possibly due to the improved donor ability and diminished steric strain of the trimethylphosphine ligands, which outweigh the stability associated with the macrocyclic complex.

Complex **6** was synthesised according to a similar method reported by Wieghardt [25]. As in the synthesis

Table 1
X-ray crystallographic data for compounds **1**, **2**, **3** and **6**

	1	**2**	**3**	**6**
Chemical formula	$C_{24}H_{44}N_8Cl_4Fe_2O_3$	$C_{19}H_{40}N_6Cl_6Fe_2O$	$C_{53}H_{74}N_8Cl_{10}OP_2Ru_2$	$C_{15}H_{28}N_4Cl_4ORuS$
Formula weight	746.17	692.97	1457.78	562.34
Crystal system	monoclinic	triclinic	triclinic	monoclinic
Space group	$P2_1/n$	$P\bar{1}$	$P\bar{1}$	$C2/c$
a (Å)	18.1197(3)	9.5812(4)	10.3558(1)	25.7902(7)
b (Å)	9.7776(2)	11.1007(3)	15.7597(1)	9.4621(3)
c (Å)	19.6919(5)	14.6649(9)	20.7427(2)	21.4965(3)
α (°)	90	81.148(2)	110.9151(4)	90
β (°)	107.3660(10)	75.641(2)	100.1199(4)	116.605(2)
γ (°)	90	77.059(2)	93.4982(7)	90
Volume (Å^3)	3329.73(12)	1464.62(9)	3084.90(5)	4690.30(2)
Z	4	2	2	8
Temperature (K)	150(2)	150(2)	150(2)	150(2)
Absorption coefficient (mm^{-1})	1.231	1.562	1.019	1.228
Total data collected	32672	14448	64679	11930
Unique data	6518 [$R_{int} = 0.0881$]	5729 [$R_{int} = 0.0499$]	14,137 [$R_{int} = 0.0885$]	4439 [$R_{int} = 0.0881$]
Observed data	5580 [$I > 2\sigma(I)$]	5121 [$I > 2\sigma(I)$]	12,232 [$I > 2\sigma(I)$]	3919 [$I > 2\sigma(I)$]
$R_1[I > 2\sigma(I)]$	0.0497	0.0331	0.0382	0.0648
$wR_2[I > 2\sigma(I)]$	0.1367	0.0791	0.0984	0.1815

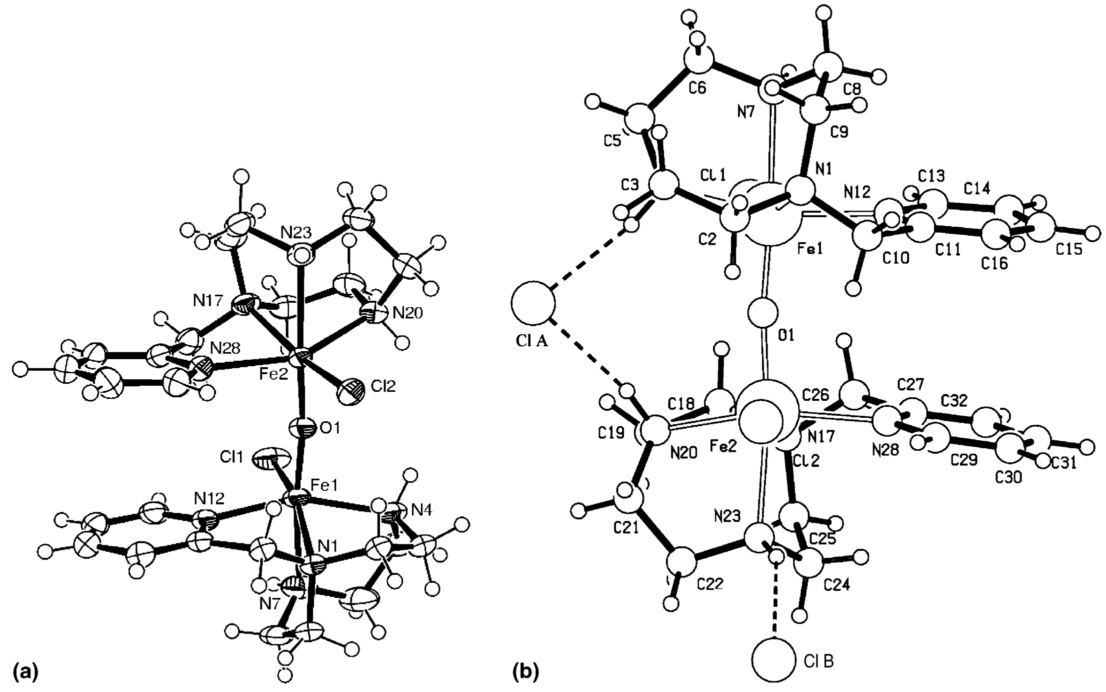

Fig. 1. (a) A view of **1** without hydrogen bonding with 50% probability ellipsoids and anions excluded, (b) a view of **1** with hydrogen bonding and the chloride anions included.

of **3**, stirring at room temperature did not yield the desired complex. When the reaction was performed at 110 °C, a yellow solid was precipitated, as observed in Scheme 3. The solid was isolated by filtration and extracted into dichloromethane. The dichloromethane extracts were filtered from a thick black solid. The extracts were concentrated to a minimum volume, whereupon addition of diethyl ether precipitated a yellow residue. The compound was characterised by NMR spectroscopy, mass spectrometry and X-ray crystallography. A satisfactory elemental analysis was not obtained, this is thought to be due to residual dimethylsulfoxide which could not be removed despite repeated washing.

Table 2
Selected bond lengths and angles for complex **1**

Bond	Length (Å)
Fe(1)–N(1)	2.285(2)
Fe(1)–N(2)	2.193(2)
Fe(1)–N(3)	2.199(2)
Fe(1)–Cl(1)	2.4058(6)
Fe(1)–Cl(2)	2.3581(6)
Fe(1)–O(1)	1.7913(14)
Fe(2)–N(4)	2.277(2)
Fe(2)–N(5)	2.176(2)
Fe(2)–N(6)	2.240(2)
Fe(2)–Cl(3)	2.3834(6)
Fe(2)–Cl(4)	2.3580(6)
O(1)–Fe(2)	1.7839(14)
	Angle (°)
N(3)–Fe(1)–N(1)	76.92(7)
N(2)–Fe(1)–N(3)	76.66(7)
N(2)–Fe(1)–N(1)	78.02(6)
Cl(2)–Fe(1)–Cl(1)	95.27(2)
Fe(2)–O(1)–Fe(1)	156.89(9)
N(6)–Fe(2)–N(4)	76.89(7)
N(5)–Fe(2)–N(6)	77.21(7)
N(5)–Fe(2)–N(4)	78.09(7)
Cl(4)–Fe(2)–Cl(3)	97.99(2)
Average bond lengths and angles	
Average Fe–N (Å)	2.29
Average Fe–Cl (Å)	2.38
Average Fe–O (Å)	1.79
Average N–Fe–N (°)	77.30
Average Cl–Fe–Cl (°)	96.63

Estimated standard deviations are given in parentheses.

2.2. Crystallography

The crystallographic details for compounds **1**, **2**, **3** and **6** are given in Table 1. Complex **1** crystallised in the space group $P2_1/n$. The molecular structure of **1** can be seen in Fig. 1(a) and the relevant bond lengths are given in Table 2. There is one molecule of the complex **1** per asymmetric unit and four molecules per unit cell. Also present in the asymmetric unit are two molecules of water, one of which is found to be disordered. The presence of the water is accounted for by the fact that the compound was recrystallised from ‘wet’ solvents. The general structure is that of two distorted octahedra linked by a bridging oxygen atom. The triazacyclononane ring occupies three of the co-ordination sites in a facial manner and the pendant pyridine moiety, a fourth. For the oxygen bridge to be incorporated into the structure, however, one of the chloride ligands is displaced. This displacement gives the complex an overall 2+ charge, balanced by the two chloride counter ions. From the molecular structure of **1** it can be seen that the pendant pyridine rings appear to lie directly above each other, in a parallel fashion. Analysis of the structure reveals that the centroids of the two rings are 3.862 Å apart, further than the sum of the van der Waals radii.

Three hydrogen bonds are apparent in the structure, existing between the N–H units of the triazacyclononane ring and the chloride anions, which is shown in Fig. 1(b) and the data for the H-bond is given in Table 3. The positions of these anions are the key to the overall geometry of the structure. Two chloride ions are present in the structure, Cl(A) and Cl(B). Cl(A) is positioned between the two (tacn)Fe units. Two hydrogen bonds link the chloride ion to the two triazacyclononane units,

Table 3
Selected bond lengths and angles for the H-bonding interactions for complexes **1**, **2** and **3**

D–H···A	D–H (Å)	H···A (Å)	D···A (Å)	Angle (°)
1				
N2–H2···Cl3	0.93	2.616	3.373	138.9
N3–H3···Cl4	0.93	2.406	3.196	142.6
2				
N4–H4···Cl2	0.93	2.295	3.209	167.3
N20–H20···Cl2	0.93	2.323	3.219	161.7
N23–H23···Cl1	0.93	2.495	3.320	147.8
3				
N2–H2···O1	0.930	2.048	2.967	169.56
O1–H2W···Cl12	0.866	2.351	3.180	160.54
N3–H3···Cl12	0.930	2.429	3.256	148.04

N(4)–H(4)···Cl(A) and N(20)–H(20)···Cl(A) forming an intramolecular bridge. It is probably this bridge which holds the molecule in its distinctive arrangement, rather than any interaction between the two pyridine rings. A second, weaker type of hydrogen bond links the other chloride anion to the cation, N(23)–H(23)···Cl(B) (Fig. 4). Unfortunately, because the water molecules in the structure are disordered and the hydrogen atoms were not located, determination of any further hydrogen bonding was not possible.

Complex **2** crystallised in the space group $P\bar{1}$. The molecular structure of **2** can be seen in Fig. 2(a) and the relevant bond lengths are given in Table 4. There are two molecules of the compound per unit cell and one molecule of dichloromethane per molecule of complex. The general structure is that of two slightly distorted octahedra of $LFeCl_2$ molecules linked by a bridging oxygen atom which occupies the remaining co-ordination site of the metal centre. The average Fe–N bond for the secondary amino groups is 2.202 Å, whereas for the

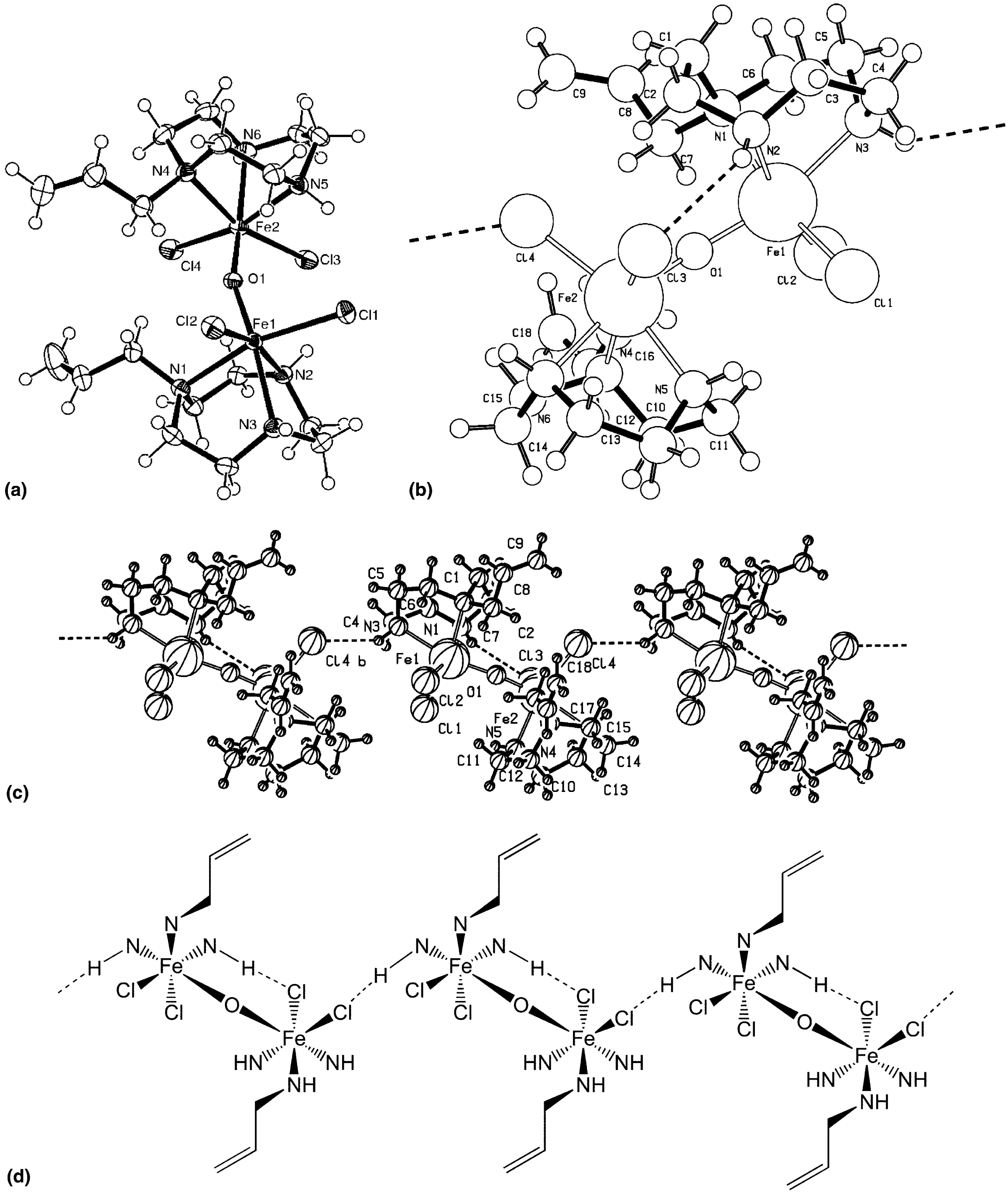

Fig. 2. (a) A view of **2** without hydrogen bonding with 50% probability ellipsoids, (b) a representation of the intra- and intermolecular hydrogen bonding in **2**, (c) the intermolecular hydrogen bonding linking molecules of **2** in a chain and (d) a schematic representation of **2** (c).

Table 4
Selected bond lengths and angles for complex **2**

Bond	Length (Å)
Fe(1)–N(1)	2.199(3)
Fe(1)–N(4)	2.137(3)
Fe(1)–N(7)	2.256(3)
Fe(1)–N(12)	2.147(3)
Fe(1)–Cl(1)	2.3427(9)
Fe(1)–O(1)	1.797(2)
Fe(2)–N(17)	2.214(2)
Fe(2)–N(20)	2.151(2)
Fe(2)–N(23)	2.280(2)
Fe(2)–N(28)	2.183(2)
Fe(2)–Cl(2)	2.3157(8)
O(1)–Fe(2)	1.802(2)
	Angle (°)
N(4)–Fe(1)–N(1)	79.93(10)
N(4)–Fe(1)–N(7)	77.72(12)
N(1)–Fe(1)–N(7)	77.01(11)
N(12)–Fe(1)–N(1)	76.06(9)
Fe(1)–O(1)–Fe(2)	173.23(13)
N(20)–Fe(2)–N(17)	79.51(10)
N(17)–Fe(2)–N(23)	76.89(9)
N(20)–Fe(2)–N(23)	76.80(10)
N(28)–Fe(2)–N(17)	75.84(10)
Average bond lengths and angles	
Fe–N(tacn) (Å)	2.206
Fe–N(py) (Å)	2.165
N–Fe–N(tacn) (°)	77.98
Fe–Cl (Å)	2.3292
Fe–O (Å)	1.80

Estimated standard deviations in parentheses.

tertiary amino groups, the average Fe–N bond length is 2.282 Å. These differ from [(Me$_3$tacn)FeCl$_2$]$_2$(μ-O) [26] and [(tacn)Fe(acac)]$_2$(μ-O)(ClO$_4$)$_2$ [27], where the longer Fe–N bonds *trans* to the oxygen atom, with values of 2.414(4) and 2.229(6) Å, respectively.

The Fe(1)–O–Fe(2) angle is 156.89(9)° is comparable to that found for [(tacn)Fe(acac)]$_2$(μ-O)(ClO$_4$)$_2$, where Fe–O–Fe is 158.6(3)° [27]. Surprisingly, this angle is very different from an analogous compound [(Me$_3$tacn)-FeCl$_2$]$_2$(μ-O) [26], which has a Fe–O–Fe of 180°. A possible explanation for this can be found when a PLATON analysis [28] of **2** is carried out. This reveals the existence of two hydrogen bonds in the lattice (Table 3) and is shown in Fig. 2(b). Of the two bonds, one is a weak intramolecular bond, N(2)–H(2)···Cl(3), forming a bridge between the two tacn iron units. This could be the reason for the Fe(1)–O–Fe(2) angle is 156.89(9)°. On comparison with [(tacn)Fe(acac)]$_2$(μ-O)(ClO$_4$)$_2$ (examined on the CCDC database) with an Fe–O–Fe angle of 158.6(3)°, it is possible that there is H-bonding from the tacn with the (ClO$_4$)$_2$, but it is difficult to determine due to the disorder associated with the anion [27]. The other

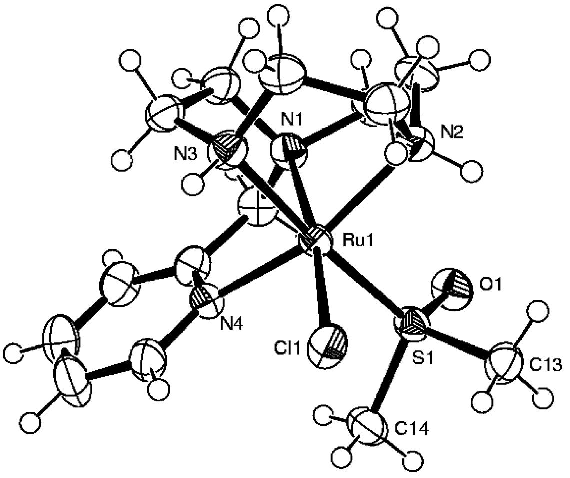

Fig. 4. A view of **6** with 50% probability ellipsoids and anion excluded.

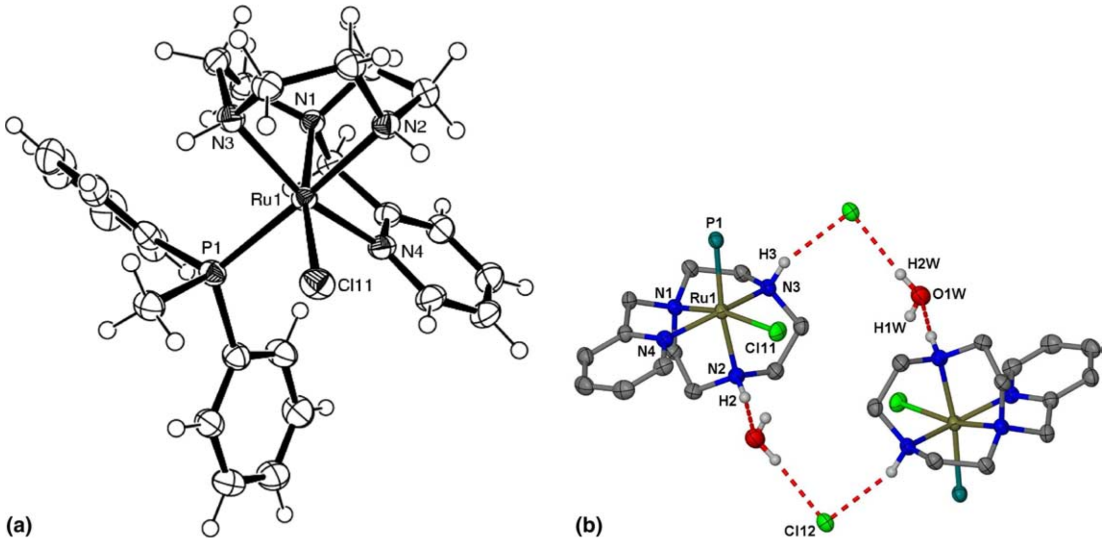

Fig. 3. (a) A view of **3** without hydrogen bonding with 50% probability ellipsoids, (b) a representation of the intra- and intermolecular hydrogen bonding in **3**.

Table 5
Selected bond lengths and angles for complex **3**

Molecule 1	Molecule 2
Bond	Length (Å)
Ru(1)–N(1)	2.089(2)
Ru(1)–N(2)	2.154(2)
Ru(1)–N(3)	2.117(2)
Ru(1)–N(4)	2.067(2)
Ru(1)–Cl(11)	2.4510(6)
Ru(1)–P(1)	2.3045(6)
P(1)–C(13)	1.835(3)
Ru(2)–N(5)	2.085(2)
Ru(2)–N(6)	2.138(2)
Ru(2)–N(7)	2.122(2)
Ru(2)–N(8)	2.056(2)
Ru(2)–Cl(21)	2.4568(6)
Ru(2)–P(2)	2.3016(6)
P(2)–C(38)	1.827(3)
	Angle (°)
N(1)–Ru(1)–N(2)	80.65(8)
N(2)–Ru(1)–N(3)	80.59(8)
N(1)–Ru(1)–N(3)	82.72(8)
N(1)–Ru(1)–N(4)	81.50(8)
N(4)–Ru(1)–P(1)	95.09(6)
N(4)–Ru(1)–Cl(11)	96.31(6)
N(5)–Ru(2)–N(6)	81.55(6)
N(6)–Ru(2)–N(7)	81.18(8)
N(5)–Ru(2)–N(7)	83.89(8)
N(5)–Ru(2)–N(8)	80.60(8)
N(8)–Ru(2)–P(2)	91.55(6)
N(8)–Ru(2)–Cl(21)	96.21(6)

Estimated standard deviations in parentheses.

H-bond is a stronger intermolecular bond, N3–H3···Cl4, forming a link from the N–H unit of a tacn unit to the adjacent molecule. These hydrogen bonds link the individual complexes into a chain. The complexes in the chain are related to each other by translation (Figs. 2(c) and (d)). There are no hydrogen bonding interactions between the chains, however, the chains pack together in a specific manner. As the units of the chain are linked together by translation, the pendant arms are situated on the same face of the molecule and the chains pack with these faces adjacent to each other. The solvent molecules are found in the cavity between the tacn faces. Thus, there is a hydrophilic interior to the chains of sandwiched **2** molecules and the hydrophobic exterior of propene pendant arms does not allow for hydrogen bonding between the chains.

Single orange needles suitable for X-ray crystallographic analysis were grown by the diffusion of diethyl ether vapour into a dichloromethane solution of **3** at room temperature over a period of several days. Complex **3** crystallised in the space group $P\bar{1}$. There are four molecules of **3**, six molecules of dichloromethane and two molecules of adventitious water in the unit cell; therefore the asymmetric unit of **3** contains two molecules of complex, three molecules of solvent and one molecule of water. Selected bond lengths and angles can be found in Table 4.

A change of a PPh_3 group to a PPh_2Me ligand has a profound effect on the geometry of the resultant ruthenium complex with respect to disposition of the ligands with respect to each other, as well as Ru–N bond lengths. Thus, the phosphine in **3** lies *trans* to the substituted nitrogen of the functionalised tacn whereas a chloride takes this position for {chloro(triphenylphosphine)[κ^4-1-(2-methylpyridyl)-1,4,7-triazacyclononane]ruthenium(II)}-chloride [19]. All three ruthenium–nitrogen tacn skeleton bond distances are markedly different for complex **3**, whereas for the PPh_3 derivative they are of a very similar length with an average Ru–N bond distance of 2.12 Å. The Ru–N distance which is *trans* to the chloride ligand has the shortest bond length (Ru(1)–N(1) = 2.09 Å), presumably due to the *trans* influence of the chloride ligand. It is also notable the longest bond length of the three is the one which lies *trans* to the phosphine ligands (Ru(1)–N(2) = 2.15 Å).

The adventitious water molecule plays an important role in the crystal packing of this particular structure. A diagram illustrating this hydrogen bonding can be seen in Fig. 3(b). The hydrogen bonded network involves only one molecule of the asymmetric unit, along with the associated counter-anion and water molecule. Through the inversion symmetry associated with the $P\bar{1}$ space group, the symmetry equivalent molecule is generated

Table 6
Selected bond lengths and angles for complex **6**

Bond	Length (Å)	Vector	Angle (°)
Ru(1)–N(1)	2.071(4)	N(1)–Ru(1)–N(2)	83.63(18)
Ru(1)–N(2)	2.100(4)	N(2)–Ru(1)–N(3)	81.32(17)
Ru(1)–N(3)	2.130(4)	N(1)–Ru(1)–N(3)	81.49(17)
Ru(1)–N(4)	2.082(4)	N(1)–Ru(1)–N(4)	80.32(16)
Ru(1)–Cl(1)	2.4434(12)	N(4)–Ru(1)–Cl(1)	96.799(12)
Ru(1)–S(1)	2.2416(12)	N(2)–Ru(1)–S(1)	94.17(12)
S(1)–O(1)	1.494(4)	Cl(1)–Ru(1)–S(1)	90.16(15)
S(1)–C(13)	1.779(6)		
S(1)–C(14)	1.787(5)		

Estimated standard deviations in parentheses.

and the hydrogen bonding is shown. The general structural motif is that of a 'dimeric' complex.

The amine proton H2 hydrogen bonds to the oxygen atom O1W′ with a bond length of 2.048 Å (all hydrogen bond lengths can be seen in Table 2). The proton associated with this water molecule H2W′ is involved in a hydrogen bond interaction with the chloride anion Cl12 with H–Cl distance determined as 2.351 Å. The final part of this network involves a further N–H–Cl interaction between Cl12 and the amine proton H3′ of the symmetry generated molecule 1′ of the asymmetric unit. A hydrogen bond is also observed between the second counter-anion and the macrocyclic ring of the second molecule of the asymmetric unit, N7–H7–Cl22. The bond distance as determined by PLATON [28] is 2.609 Å.

Single crystals of complex **6** were obtained as yellow blocks from a dichloromethane/diethyl ether solution which was stored at −20 °C for several months. The complex crystallised in the monoclinic space group *C*2/c, and there are therefore eight molecules of the complex in the unit cell, along with eight molecules of dichloromethane. The molecular structure can be seen in Fig. 4 and selected bond lengths and angles can be seen in Tables 5 and 6. These values are typical of other complexes determined in this area. There are many ruthenium DMSO complexes which have been structurally characterised by crystallography, and though many of these contain a sulfur-bound dimethylsulfoxide ligand, there are few in which can be directly compared with this donor ligand set, that is "RuCl(DMSO)N_4" [29–32].

3. Conclusion

The oxidation of functionalised (tacn)Fe(II) complexes has been carried out in a controlled fashion to lead to dramatically different types of μ-oxo(tacn)Fe(III) complexes, depending on the binding capability of the pendant arm. The dimeric complexes produced show interesting and different types of hydrogen bonding interactions in the solid state. Also, a number of new functionalised and unfunctionalised tacn Ru(II) complexes have been synthesised and structural studies carried out.

4. Experimental

Standard inert atmosphere techniques were used throughout, where appropriate. Solvents were stored over appropriate pre-drying agents and distilled under N_2. Dichloromethane was distilled from CaH_2, THF was distilled from potassium, toluene and petroleum ether (b.p. 40–60 °C) were distilled from sodium and diethyl ether was distilled from Na/Ph_2CO. NMR solvents were degassed by three freeze–pump–thaw cycles and stored over 4 Å molecular sieves in a dry box, except D_2O. All reagents were purchased in reagent grade and used without further purification. ^{1}H, ^{13}C{^{1}H} and ^{31}P NMR spectra were recorded on Bruker 250 and 500 MHz NMR spectrometers. IR spectra were recorded on a Perkin–Elmer 1600 spectrometer. Mass spectrometry was performed by the University of Leeds Mass Spectrometry Service. Elemental analyses were performed by the University of Leeds Microanalytical Services. 1,4,7-triazacyclononane [34], 1-(2-methylpyridyl)-1,4,7-triazacyclononane [20], and 1-(propene)-4,7-triazacyclononane [35], $RuCl_2(PPh_2Me)_4$ [36], $RuCl_2(PPhMe_2)_4$ [37], and $RuCl_2(DMSO)_4$ [33] were prepared by literature procedures.

4.1. [bis(1-(2-methylpyridyl)-1,4,7-triazacyclononane iron(III)chloride)μ-oxo]Dichloride (1)

[1-(2-methylpyridyl)-1,4,7-triazacyclononane]Iron(II)-dichloride (0.342 g, 0.0008 mol) was dissolved in dichloromethane (50 ml). The solution was stirred in air overnight, during which time a brown solid was seen to precipitate. The resulting suspension was then filtered and the solid dried. (0.312 g, 0.00035 mol, 89%). Recrystallisation from ethanol/diethyl ether afforded **1** as red plates. Found: C, 38.5; H, 6.0; N, 14.8; Cl, 19.2%. Calc. for $C_{24}N_8H_{40}Fe_2Cl_4O.2H_2O$: C, 38.6; H, 5.9; N, 15.0; Cl, 19.0%.

4.2. Bis[1-(propene)-4,7-triazacyclononane iron(III)dichloride]oxide (2)

To a suspension of anhydrous iron(II)chloride (0.894 g, 0.0071 mol) in THF (50 ml) was added a solution of 1-(propene)-4,7-triazacyclononane (1.312 g, 0.0078 mol) in THF (20 ml). The resulting suspension was heated to reflux for 7 days. After this time the THF was removed under reduced pressure. The remaining solid was extracted with dichloromethane to give a dark green powder. Recrystallisation from dichloromethane/petrol afforded **2** as green crystals (1.22 g, 0.0019 mol, 56%). Found: C, 33.0; H, 5.9; N, 12.1; Cl, 30.5%. Calc. for $C_{18}H_{38}N_6Fe_2Cl_4O.CH_2Cl_2$: C, 32.9; H, 5.8; N, 12.1; Cl, 30.7%.

4.3. [chloro(methyldiphenylphosphine){κ^4-1-(2-methylpyridyl)-1,4,7-triazacyclononane}ruthenium(II)]chloride (3)

To a Schlenk tube charged with a solution of $RuCl_2(PMePh_2)_4$ (0.250 g, 0.00026 mol) in toluene (10 ml) was added 1-(2-methylpyridyl)-1,4,7-triazacyclononane (0.085 g, 0.00039 mol). The resulting green solution was heated to reflux temperature for 1 h. After this time, a yellow solid was observed to have precipitated. The suspension was concentrated to ca. 5 ml, and petrol added, resulting in further precipitation of a yellow solid. The solid was isolated by filtration, washed with petrol, and dried in vacuo. Recrystallisation was achieved by diffusion of diethyl ether vapour into a dichloromethane solution at room temperature. (0.131 g, 0.00022 mol, 84%). Found: C, 49.8; H, 5.5; N, 9.4%. Calc. for $C_{25}H_{33}N_4Cl_2PRu$: C, 50.6; H, 5.6; N, 9.5%. ^1H NMR (300.13 MHz, $CDCl_3$, 298 K): 1.82 (d, 3H, $P(C_6H_5)_2(CH_3)$, $^2J(^1H–^{31}P) = 7.9$ Hz), 1.95 (m, 1H, N–CH_2 ring), 2.57 (m, 1H, N-CH_2 ring), 3.05 (m, 1H, N-CH_2 ring), 3.21 (d, 1H, N-CH_2 arm, $^2J(^1H–^1H) = 15$ Hz), 3.32–3.60 (m, 8H, N-CH_2 ring), 3.86 (m, 1H, N-CH_2 ring), 4.40 (d, 1H, N-CH_2 arm, $^2J(^1H–^1H) = 15$ Hz), 4.45 (s, br, 1H, N-*H*), 5.20 (s, br, 1H, N-*H*), 7.17–7.62 (m, complex, 13H, 10H of $P(C_6H_5)_2(CH_3)$ and 3H, C*H* of py, overlap) 9.02 (d, 1H, C*H* of py, $^3J(^1H–^1H) = 4.8$ Hz).

^{13}C NMR (62.90 MHz, $CDCl_3$, 298 K): 15.2 (d, $P(C_6H_5)_2(CH_3)$, $^1J(^{31}P–^{13}C) = 31.6$ Hz), 45.5, 51.1, 53.1, 54.1, 60.8, 62.7 (6s, N-CH_2 ring), 69.4 (N-CH_2 arm), 122.3, 124.2 (2s, *C*H of py), 128.9, 129.1, 129.8, 129.9 (all s, $P(C_6H_5)_2(CH_3)$), 134.7, 153.2 (2s, *C*H of py), 165.3 (s, quaternary of py). ^{31}P NMR: +34.7 (s, $P(C_6H_5)_2(CH_3)$). MS (ES): 557.4 ($[M^+] - Cl$).

4.4. [chloro(methyldiphenylphosphine)-1,4,7-triazacyclononane]ruthenium(II)chloride (4)

To a Schlenk tube charged with a solution of $RuCl_2(PMePh_2)_4$ (0.25 g, 0.00026 mol) in toluene (30 ml) was added 1,4,7-triazacyclononane (0.033 g, 0.00026 mol). The resulting green solution changed colour immediately to yellow. The suspension was concentrated to ca. 5 ml, and petrol added, resulting in further precipitation of a yellow solid. The solid was isolated by filtration, washed with petrol, and dried in vacuo. Recrystallisation was achieved by diffusion of diethyl ether vapour into a dichloromethane solution at room temperature (0.075 g, 0.00017 mol, 41%). Found: C, 55.3; H, 6.0; N, 5.7%. Calc. for $C_{32}H_{33}N_4Cl_2PRu$: C, 54.8; H, 5.9; N, 6.0%. ^1H NMR (300.13 MHz, $CDCl_3$, 298 K): 1.54 (s, br, 3H, N-*H*), 1.82 (m, 6H, $P(C_6H_5)_2(CH_3)$, 2.22 (m, 3H, N-CH_2 ring), 2.51 (m, 3H, N-CH_2 ring), 3.25 (m, 2H, N-CH_2 ring), 3.67 (m, 2H, N-CH_2 ring), 3.90 (m, 2H, N-CH_2 ring), 7.17 (m, 8H, $P(C_6H_5)_2(CH_3)$), 7.45 (m, 4H, $P(C_6H_5)_2(CH_3)$), 7.55 (m, 4H, $P(C_6H_5)_2(CH_3)$), 7.86 (m, 4H, $P(C_6H_5)_2(CH_3)$); $^{13}C\{^1H\}$ NMR (62.90 MHz, $CDCl_3$, 298 K): 13.4 (d, $P(C_6H_5)_2(CH_3)$), $^1J(^{31}P–^{13}C) = 26.4$ Hz), 48.6, 49.4, 53.5 (3s, N-CH_2 ring), 69.4 (N-CH_2 arm), 128.4, 128.8, 128.9, 129.5, 130.3, 132.1 (all s, $P(C_6H_5)_2(CH_3)$); $^{31}P\{^1H\}$ NMR (101.26 MHz, $CDCl_3$, 298 K): 27.3 (s, $2P(C_6H_5)_3$). MS (ES): 666.8 ($[M^+] - Cl$).

4.5. [chloro(bis-dimethylphenylphosphine)-(1,4,7-triazacyclononane)ruthenium(II)chloride] (5)

To a Schlenk tube charged with a solution of $RuCl_2(PMe_2Ph)_4$ (0.15 g, 0.00019 mol) in toluene (30 ml) was added 1,4,7-triazacyclononane (0.024 g, 0.00026 mol). The orange solution was stirred for 12 h and darkened in colour with a yellow solid present. The suspension was concentrated to ca. 5 ml, and petrol added, resulting in further precipitation of a yellow solid. The solid was isolated by filtration, washed with petrol, and dried in vacuo. Recrystallisation was achieved by diffusion of diethyl ether vapour into a dichloromethane solution at room temperature (0.030 g, 0.000053 mol, 27%). Found: C, 47.1; H, 6.5; N, 7.3%. Calc. for $C_{32}H_{33}N_4Cl_2PRu$: C, 45.7; H, 6.5; N 7.3%. ^1H NMR (500.13 MHz, $CDCl_3$, 298 K): 1.56 (s, br, 3H, N-*H*), 1.64 (m, 6H, $P(CH_3)_2(C_6H_5)$, $^2J(^1H–^{31}P) = 3.6$ Hz), 2.07 (m, 6H, $P(CH_3)_2(C_6H_5)$, $^2J(^1H–^{31}P) = 3.6$ Hz), 2.19 (m, 2H, N-CH_2 ring), 2.34 (m, 2H, N-CH_2 ring), 2.43 (m, 2H, N-CH_2 ring), 2.84 (m, 2H, N-CH_2 ring), 3.51 (m, 3H, N-CH_2 ring), 7.12 (m, 1H, $P(CH_3)_2(C_6H_5)$), 7.22 (m, 4H, $P(CH_3)_2(C_6H_5)$), 7.41 (m, 4H, $P(CH_3)_2(C_6H_5)$), 7.78 (m, 4H, $P(CH_3)_2(C_6H_5)$); $^{13}C\{^1H\}$ NMR (62.90 MHz, $CDCl_3$, 298 K): 17.4 (d, $P(CH_3)(C_6H_5)_2$, $^1J(^{31}P–^{13}C) = 26.4$ Hz), 48.5, 49.5, 53.9 (3s, N-CH_2 ring), 128.4, 128.8, 128.9, 129.5, 130.3, 132.1 (6s, $P(CH_3)(C_6H_5)_2$, $^{31}P\{^1H\}$ NMR (101.26 MHz, $CDCl_3$, 298 K): 23.6 (s, $2P(C_6H_5)_3$). MS (ES): 542.6 ($[M^+] - Cl$).

4.6. Chloro(dimethylsulfoxide)[κ^4-1-(2-methylpyridyl)-1,4,7-triazacyclononane]ruthenium(II)chloride (6)

To a Schlenk tube charged with a suspension of $RuCl_2(DMSO)_4$ (2.50 g, 0.0052 mol) in toluene (50 ml) was added 1-(2-methylpyridyl)-1,4,7-triazacyclononane (1.19 g, 0.0054 mol). The suspension was heated to reflux temperature for 1 h. After this time, the resulting yellow solid was isolated by filtration and extracted into dichloromethane (50 ml). The dichloromethane extracts were concentrated to ca. 5 ml, and diethyl ether added, resulting in the precipitation of a bright yellow solid which was washed with diethyl ether (6 × 20 ml) and dried in vacuo. Single crystals suitable for X-ray crystallographic analysis were grown from a dichloromethane/diethyl ether solution (1.744 g 0.0037 mol, 71 %). Found: C, 32.1; H, 5.7; N, 9.5%. Calc.for $C_{14}H_{26}N_4Cl_2ORuS$: C, 35.3; H, 5.6; N, 9.6%. ^1H NMR ($(CD_3)_2SO$, 250.13 MHz, 298 K) 2.57–3.25 (m, 12H, N-CH_2 ring), 3.31–3.40 (s, 6H, $(CH_3)_2S({=}O)$-Ru), 4.59 (d of d, 2H, N-CH_2 arm, $^2J(^1H–^1H) = 14.9$ Hz), 6.02 (s, br, 1H N-*H*), 6.89 (s, br, 1H, N-*H*), 7.50 (m, 2H, C*H* of py), 7.90 (t, 1H, C*H* of py, $^3J(^1H–^1H) = 6.3$ Hz), 8.79 (d, 1H, C*H* f py, $^3J(^1H–^1H) = 5.0$ Hz). $^{13}C\{^1H\}$ NMR (62.90 MHz, $(CD_3)_2SO$, 298 K): 52.0, 53.0, 54.1, 55.5, 59.2, 61.8 (6s, N-CH_2 ring), 69.3 (s, N-CH_2 arm), 122.5, 124.5, 136.4, 147.3 (4s, *C*H of py), 165.8 (s, quaternary of py) 47.6, 48.2 (2s, $CH_3)_2S(=O)$-Ru DMSO) MS (ES): 434.8 ($[M^+] - Cl$), 356.9 ($[M^+] - Cl - DMSO$).

4.7. Crystallographic data collection and structure collection

Data for compounds **1**, **2**, **3** and **6** were collected on a Nonius KappaCCD area-detector diffractometer using graphite monochromated Mo Kα radiation ($\lambda = 0.71073$ Å) using 1.0° ϕ-rotation frames. Pertinent crystallographic details are given in Table 2.

The structures of all compounds were solved by direct methods using SHELXS 86. Refinement, by full-matrix least squares on F^2 using SHELXS 97, was similar for all four compounds. Hydrogen atoms were constrained to idealised positions using a riding model (with free rotation for methyl groups), with the exception of the hydrogen atoms of the water molecules in **3** which were located in the difference map and refined isotropically. The hydrogen atoms of the disordered water molecules of **1** were not located. All non-hydrogen atoms were refined anisotropically.

Acknowledgements

We thank Dr. Mark Thornton-Pett with help the X-ray crystallography.

References

[1] M. Fontecave, S. Menage, C. Duboc-Toia, Coord. Chem. Rev. 180 (1998) 1555.
[2] L. Que, A.E. True, Progr. Inorg. Chem. 38 (1990) 97.
[3] D.M. Kurtz, Chem. Rev. 90 (1990) 585.
[4] S. Menage, L. Que, New J. Chem. 15 (1991) 431.
[5] A. Dei, D. Gatteschi, L. Pardi, Inorg. Chem. 32 (1993) 1389.
[6] T. Funabiki, A. Mizoguchi, T. Sugimoto, S. Tada, M. Tsugi, H. Sakamoto, S. Yoshida, J. Am. Chem. Soc. 108 (1986) 2921.
[7] M. Ito, L.J. Que, Angew. Chem. Int. Ed. Engl. 36 (1997) 1342.
[8] G. Lin, G. Reid, T.D.H. Bugg, Chem. Commun. (2000) 1119.
[9] G. Lin, G. Reid, T.D.H. Bugg, J. Am. Chem. Soc. 123 (2001) 5030.
[10] K. Wieghardt, W. Herrmann, M. Koppen, I. Jibril, G. Huttner, Z. Naturforsch. B 39 (1984) 1335.
[11] B. Albela, E. Bothe, O. Brosch, K. Mochizuki, T. Weyhermuller, K. Wieghardt, Inorg. Chem. 38 (1999) 5131.
[12] T. Justel, J. Bendix, N. Metzler-Nolte, T. Weyhermuller, B. Nuber, K. Wieghardt, Inorg. Chem. 37 (1998) 35.
[13] M.N. Bell, A.J. Blake, M. Schroder, H.J. Kuppers, K. Wieghardt, Angew. Chem. Int. Ed. Engl. 26 (1987) 250.
[14] S.M. Yang, W.C. Cheng, K.K. Cheung, C.M. Che, S.M. Peng, J. Chem. Soc., Dalton Trans. (1995) 227.
[15] S.M. Yang, M.C.W. Chan, S.M. Peng, C.M. Che, Organometallics 17 (1998) 151.
[16] S.M. Yang, M.C.W. Chan, K.K. Cheung, C.M. Che, S.M. Peng, Organometallics 16 (1997) 2819.
[17] S.M. Au, S.B. Zhang, W.H. Fung, W.Y. Yu, C.M. Che, K.K. Cheung, Chem. Commun. (1998) 2677.
[18] W.C. Cheng, W.H. Fung, C.M. Che, J. Mol. Catal., A 113 (1996) 311.
[19] A.L. Gott, P.C. McGowan, T.J. Podesta, M. Thornton-Pett, J. Chem. Soc., Dalton Trans. (2002) 3619.
[20] P.C. McGowan, T.J. Podesta, M. Thornton-Pett, Inorg. Chem. 40 (2001) 1445.
[21] T. Justel, M. Muller, T. Weyhermuller, C. Kressl, E. Bill, P. Hildebrandt, M. Lengen, M. Grodzicki, A. Trautwein, B. Nuber, K. Wieghardt, Chem. Eur. J. 5 (1999) 793.
[22] T. Justel, T. Weyhermuller, K. Wieghardt, E. Bill, M. Lengen, A.X. Trautwein, P. Hildebrandt, Angew. Chem. Int. Ed. Engl. 34 (1995) 669.
[23] M. Muller, T. Weyhermuller, E. Bill, K. Wieghardt, J. Biol. Inorg. Chem. 3 (1998) 96.
[24] C. Stockheim, L. Hoster, T. Weyhermuller, K. Wieghardt, B. Nuber, J. Chem. Soc., Dalton Trans. (1996) 4409.
[25] A. Geilenkirchen, P. Neubold, R. Schneider, K. Wieghardt, U. Florke, H.J. Haupt, B. Nuber, J. Chem. Soc., Dalton Trans. (1994) 457.
[26] A.C. Moreland, T.B. Rauchfuss, Inorg. Chem. 39 (2000) 3029.
[27] K. Wieghardt, K. Pohl, U. Bossek, B. Nuber, J. Weiss, Z. Naturf. Sect. B J. Chem. Sci. 43 (1988) 1184.
[28] A.L. Spek, Utrecht University, 2001.
[29] D. Hesek, Y. Inoue, S.R.L. Everitt, H. Ishida, M. Kunieda, M.G.B. Drew, J. Chem. Soc., Dalton Trans. (1999) 3701.
[30] T. Kojima, T. Amano, Y. Ishii, M. Ohba, Y. Okaue, Y. Matsuda, Inorg. Chem. 37 (1998) 4076.
[31] M. Yamaguchi, H. Kousaka, T. Yamagishi, Chem. Lett. (1997) 769.
[32] Y.X. Wang, D.M. Eichhorn, N. Goswami, Q. Zhao, D.P. Rillema, J. Chem. Cryst. 27 (1999) 277.
[33] I.P. Evans, A. Spencer, G. Wilkinson, J. Chem. Soc., Dalton Trans. (1973) 204.
[34] K. Wieghardt, K. Schmidt, B. Nuber, J. Weiss, Chem. Ber. 112 (1979) 2220.
[35] L.J. Farrugia, P.A. Lovatt, R.D. Peacock, Inorg. Chim. Acta 246 (1996) 343.
[36] P.W. Armit, A.S.F. Boyd, T.A. Stephenson, J. Chem. Soc., Dalton Trans. (1975) 1663.
[37] D.J. Cole-Hamilton, D.S. Chappell, A.M. Galas, M.B. Hursthouse, J. Chem. Soc., Dalton Trans. (1982) 1867.